- Technical Paper -

IMPACT OF DEMOLDING AGE AND MINERAL COMPOSITION OF CEMENT ON DRYING SHRINKAGE OF CEMENT PASTE

Tatsuya HAJI[*1], Shu KOTERA[*1], Ryo KURIHARA[*1], and Ippei MARUYAMA[*2]

ABSTRACT

Drying shrinkage of cement paste, which is affected by the age of start of drying and mineral composition of used cement, is investigated. Based on the shrinkage strain measurement and XRD/Rietveld analysis, a linear relationship between amount of amorphous phase and drying shrinkage is confirmed. But those relationships were not consistent among different cement. The reason of the different trend can be explained by the ratio of amount of portlandite to amount of amorphous, because portlandite is expected to restrain the colloidal agglomeration of amorphous.

Keywords: age at start of drying, drying shrinkage, cement paste, early demolding

1. INTRODUCTION

Curing process is crucial to make the concrete satisfying required performance, such as strength and durability. On the contrary, economical condition demands the early-age demolding because it shortens construction time. In Japanese law, especially focusing on architectural building, demolding timing and timing for removal of slab supports are determined by the concrete strength [1,2], while the other physical properties, such as durability for carbonation or salt attack is also important performance for service life of concrete structures.

Drying shrinkage of concrete is not affected by age of start of drying much [3], but drying shrinkage of hardened cement paste has important roles on the quality of concrete. Because, the drying shrinkage of paste in concrete produce micro-cracks around coarse aggregates [4] and such micro-cracks affect the gas permeability [5], diffusion coefficient [6], Young's modulus, and compressive strength [7].

In order to control the quality of concrete, especially about the cover concrete, fundamental scientific knowledge on shrinkage of cement paste which is affected by the commencement of drying is necessary. Based on this background, an experimental program about this issue was conducted.

2. EXPERIMENTAL PROGRAM

2.1 Materials

In this experimental program, Porttland cement paste is focused. Ordinary Portland cement (N) which has relatively large amount of alite with ca 5% inorganic powder allowed by JIS, and low heat Portland cement (L) are used for comparison. Properties and characteristics of those are summarized in Tables 1 and 2.

The water-cement ratio was 0.55, and the paste (10 L) was mixed in a 20 L Hobart mixer for 3 min after the water was added, and then for a further 3 min after the paste was scraped from the mixer. All the materials were stored in a thermostatic room at 20 ± 1 °C for 1 day prior to mixing. The mixing was performed at room temperature and the specimens were then immediately moved to a thermostatic room. To minimize segregation, the paste was remixed every 30 min for 6 h. The specimen size was 3 × 13 × 300 mm with steel mold.

The specimens were placed in a thermostatic

Table 1 Characteristics of cement

Cement	Notation	Properties
L Cement	L	Low heat Portland cement, density: 3.22 g/cm^3
N Cement	N	Ordinary Portland cement, density: 3.16 g/cm^3

Table 2 Mineral composition determinedby X-ray/Rietvelt analysis*

Mineral	C_3S (mass %)	C_2S (mass %)	C_3A (mass %)	C_4AF (mass %)	Periclase (mass %)	Bassanite (mass %)	Gypsm (mass %)	Calcite (mass %)
L	20.11±1.59	62.94±1.14	1.95±0.42	10.70±0.59	0.51±0.21	2.43±0.36	1.11±0.62	0.21±0.54
N	58.37±3.02	18.13±0.92	6.94±0.40	9.35±0.26	0.72±0.19	0.55±0.14	1.74±0.77	4.14±0.25

*The method of X-ray/Rietvelt analysis is explained at section 2.3.

*1 Graduate student, Dept. of Environmental Engineering and Architecture, Nagoya Univ., JCI Student Member
*2 Assoc. Prof. Graduate School of Environmental Engineering and Architecture, Nagoya Univ., Dr.Eng., JCI Member

chamber at a temperature of 20 ± 1 °C. They were demolded after 3 days, and then they were immersed in lime-saturated water for a given age of start of drying, and then dried under different RHs.

2.2 Drying process

Drying process of specimen is realized in the drying chamber. Each desiccant is placed in the bottom of each drying chamber (300 × 345 × 540 mm). A closed electro-magnetic air pomp is used for the closed air circuit with gas wash battles to keep the relative humidity constant. The schematic of the system is shown in Fig. 1. Closed loop contains three gas wash bottles, one of which is put adsorbents for CO_2, the others contains saline solution. Wind velocity near a tip of a tube is 0.066 m/s. In Table 3, the used salts with corresponding relative humidity are shown.

The samples were dried at 3, 7, 28, and 91 days, and notations are 3d, 7d, 28d, and 91d respectively. 3 days is a representative parameter for early-age demolding, 7 days represents the standard curing period, 28 days is for comparison for previous experimental results [i.e. 8], and 91 days should show the shrinkage strain of matured (negligible additional hydration process) cement paste.

Summary of the present research program is shown in Table 4.

2.3 Analysis

Shrinkage strain and mass change of the samples were measured at the commencement of drying and subsequent several periods (normally every 1 or 2 weeks). The specimen size for drying shrinkage and mass change were 3 × 13 × 100 mm which was cut from the sample with the size of 3 × 13 × 300 mm. The length change was measured by linear variable differential transformer (LVDT) with a precision of 0.001 mm. A 100-mm-long Fe-^{36}Ni alloy sample was used as a reference and the length difference between the samples and the reference was determined by LVDT. The length of the sample was calculated based on the length of reference. The sample deformation was divided by the original sample length to obtain the shrinkage strain. For each set of drying conditions, measurements were taken from more than five specimens. Specimen mass was measured by using a balance with a precision of 0.1 mg before and during drying.

The hcp specimens were analyzed by powder X-ray diffraction (XRD) (D8 advance, Bruker AXS) at the age of start of drying. All the hcp specimens were submerged in acetone for 6 h and dried under vacuum for several minutes with an aspirator. The specimens were stored at 11% RH and 20 °C for 2 weeks. The specimens were ground in a ball mill, and corundum powder (10 mass %) was added to the sample powder as a standard reference. The XRD conditions were as follows: tube voltage, 50 kV; tube current, 250 mA; scan range of 2θ, 5-65°; step width, 0.02°; scan speed, 2°/min. The software used for Rietveld analysis was TOPAS Ver. 4.0 (Bruker AXS). In the Rietveld analysis, the quantified phases were gypsum, bassanite, portlandite, ettringite (AFt), monosulfate (AFm), as well as typical cement minerals, such as alite (C_3S), belite (C_2S), cubic-C_3A, orthorhombic-C_3A, and C_4AF. Structural models for clinker minerals (alite, belite, cubic-C_3A, orthorhombic-C_3A, and C_4AF) were taken from an NIST Technical Report [9]. Those for calcite, gypsum, bassanite, portlandite (CH), AFt, AFm, and corundum were taken from the ICSD database [10]. After the Rietveld analysis, the degrees of hydration of the clinker minerals were calculated [11].

Table 3 Humidity table

Drug name	Humidity (RH%)
LiCl	11
KNO_2	45
NaBr	58
NH_4Cl	79

Table 4 Experiment factors

Parameter	Properties
Cement	L, N
Water cement ratio	0.55
Age at the start of drying (days)	3, 7, 28, 91
Condition of drying (% RH)	11, 45, 58, 79
Curing before drying	Under lime-saturated water
Analysis	XRD, (TG)

* ( ) is not shown in this contribution.

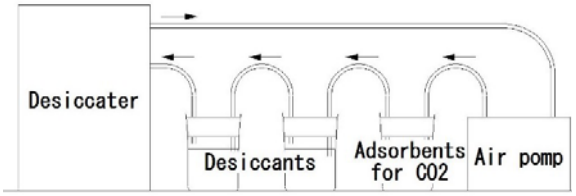

Fig. 1 Schematic the drying chamber.

3. RESULTS AND DISCUSSION

3.1 Drying shrinkage

Change in drying shrinkage of all the samples are shown in Fig. 2. According to this figure, almost all the specimens reached equilibrium state after 28 days of drying. Interestingly, the rate of drying shrinkage is not related to the strength of drying. The similar trend is also confirmed in our previous concrete and mortar specimen [12]. This is actually one of the colloidal characteristic of calcium silicate hydrates [13].

The impact of the age of drying is obvious. In Fig. 3, relationships between shrinkage strain and relative humidity affected by the age of drying is summarized. As they are shown in Fig. 3, shrinkage strain increases as the sample is matured. This trend is consistent to both N and L and the same trend was confirmed by Nagamatsu et al. [8]

The type of cement also has large impact on shrinkage strain. When the data at the same age of

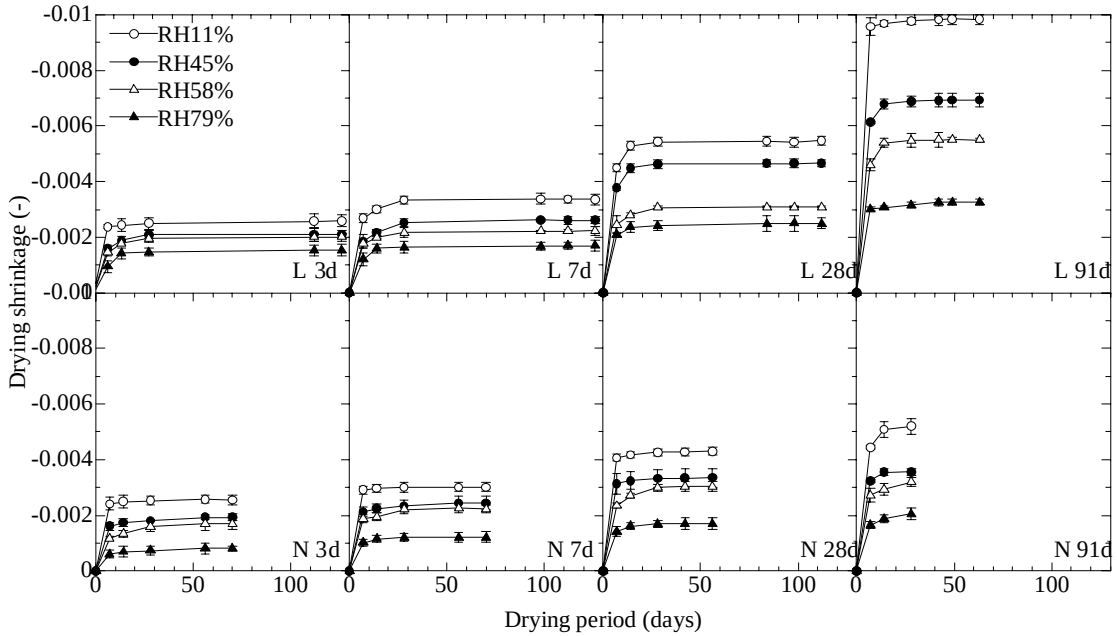

Fig. 2 Development of drying shrinkage of hardened cement pastes.

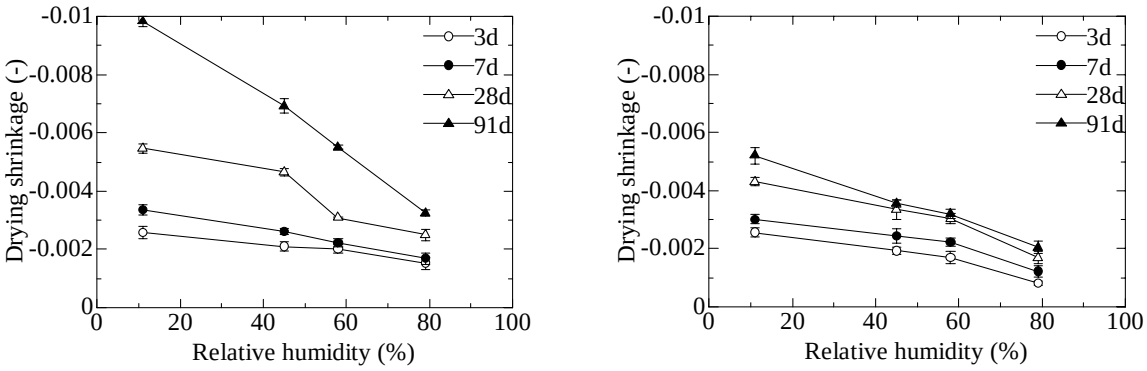

6-(a) L cement 6-(b) N cement

Fig. 3 Relationship between relative humidity, age at the start of drying, and drying shrinkage.

drying is compared, in any cases, L cement paste showed larger shrinkage strain. This trend has been confirmed in matured cement paste [14]. Especially, in case of L, incremental strain below 58% RH is larger than that of N. This tendency became significant in matured state.

3.2 Hydration and phase composition.

The difference of shrinkage strain should be resulted from the phase composition and microstructure of cement paste. Therefore, the hydration process of cement pastes was evaluated by XRD/Rietveld analysis.

The obtained development of phase compositions of L and N, calculated from the composition of the unhydrated cement and the reaction rate in Fig. 5, are summarized in Fig. 4. With regards to degree of hydration shown in Fig. 5, degree of hydration of clinker minerals are calculated from results of XRD analysis of unhydrated cement and hydrate cement. In case of L, aluminate phase attained 100% of degree of hydration after 3 days. Alite also reacts quickly and it attained about 90% degree of hydration after 7 days. On the contrary, belite and ferrite phase reacted gradually. After 91

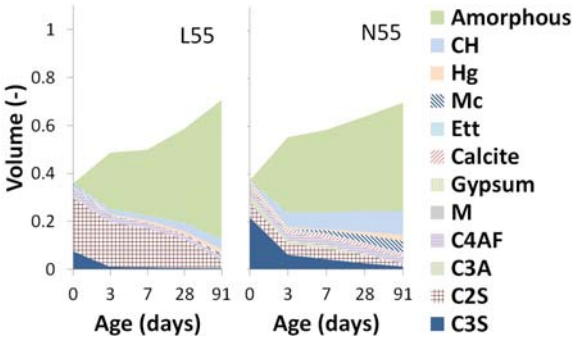

Fig. 4 Development of phase composition of L55 (right) and N55 (left). Experimental data were obtained by XRD/Rietvelt analysis.

CH: $Ca(OH)_2$, Hg: Hydrogarnet,
Mc: Monocarbonate, Ett: Ettringite, M: Periclase,
C_4AF: Ferrte phase, C_3A: Aluminate phase
C_2S: Belite, C_3S: Alite

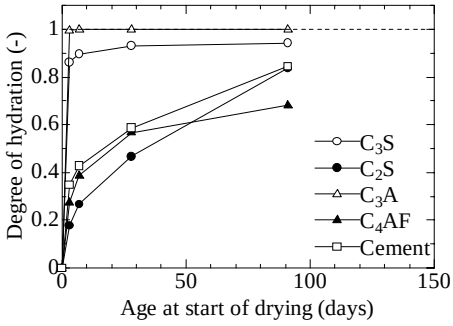

(a) L cement

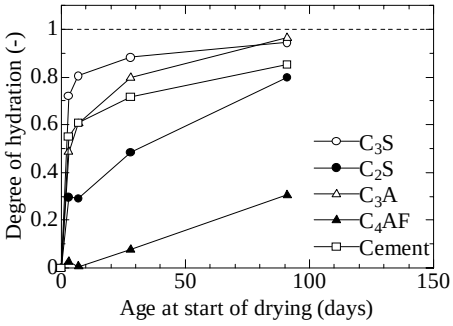

(b) N cement

Fig. 5 Degree of hydration of each clinker mineral in L (left) and N (right).

days, belite attained 80% degree of hydration.

In case of N, all the clinker mineral reacts slowly. Among them, alite reacted quickly and attained 80% degree of hydration after 7 days, and after that it reacted gradually and about 95% degree of hydration at 91 days. The belite showed the similar trend as that in case of L. After 91 days, belite reacted about 80%.

The amorphous phases, whose main component should be calcium silicate hydrates (C-S-H), in the cement paste is the most important parameters for the shrinkage of the pastes. Figure 6 shows development of amorphous phase as the time elapsed. Interestingly, N showed large amount of amorphous until 7 days, and L and N showed similar value at 28 days. At the age of 91 days, amount of amorphous phase per unit volume of L showed larger than that of N.

Large percentage of the drying shrinkage of paste under the first desorption process is irreversible, and the irreversible shrinkage is yielded from 100% RH to 40% RH [15]. Therefore, the shrinkage strain at 58% RH is representative for the shrinkage of the first drying process. In addition, many shrinkage studies have been investigated under 60% RH in Japan, therefore, there is an alibi to use the strain at 58% RH. The shrinkage strains at 58% RH are plotted as a function of the amount of amorphous phase in Fig. 7 (a). And Fig. 7 (b) shows in the case of 11% RH. As it is shown in Fig. 7 (a), shrinkage of each paste is almost linear to the amount of amorphous at the age of start of drying. But the trend is not the same. In case of drying age of 28 days, the shrinkage strains are common to L and N, but the others do not on the same trend. In case of N, even it has large amount of amorphous phase in early ages (3 days and 7 days for the age of start of drying), it showed smaller shrinkage than those of L. Therefore, the amount of amorphous is not the sole key parameter for this trend.

There are two possibilities of the reason why drying shrinkage of cement paste of L and N as a function of amorphous phase is not on the same curve. One is the amount of outer C-S-H product. Outer C-S-H, which is precipitated at the outer side of original boundary of unhydrated cement particle, has not the same characteristic as that of inner C-S-H [16]. And this outer C-S-H has an important role for

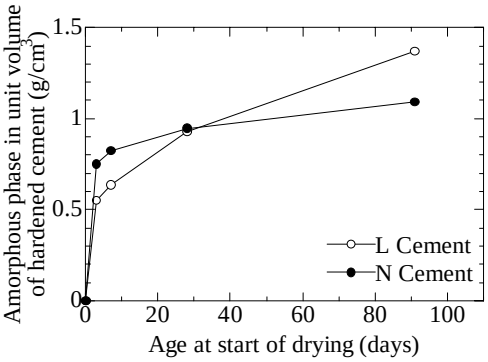

Fig. 6 Relationship between mass of amorphous phase of L and N and age at start of drying.

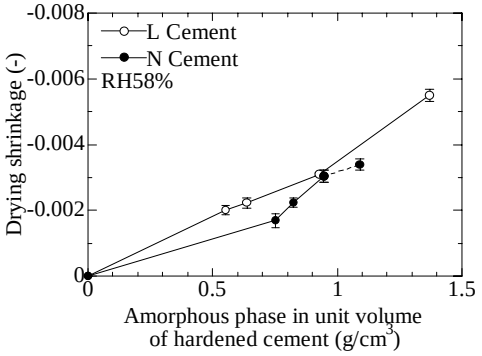

Fig. 7 (a) Relationship between mass of amorphous and drying shrinkage in RH 58%*

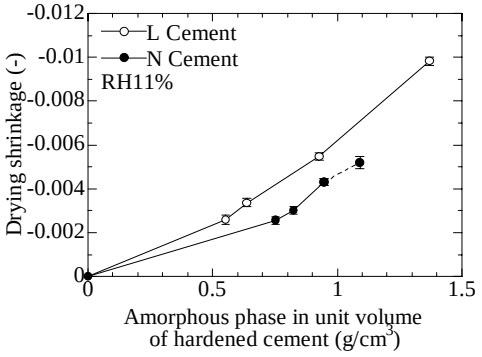

Fig. 7 (b) Relationship between mass of amorphous and drying shrinkage in RH 11%*
*The data of N_91d has not reached equilibrium.

colloidal agglomeration under the first desorption process and expected to produce the irreversible shrinkage [17]. The amount of outer C-S-H can be changed, because hydration process of alite and belite is varied in case of L and N. This is just the assumption and no additional supporting data. Further investigation is needed for clarification.

The other mechanism is concerning amount of portlandite. As it is shown in Fig. 8, there is large difference in the amount of portlandite. It has been reported that the portlandite in cement paste has an important role to restraint the shrinkage of C-S-H [18]. Consequently, the balance of (outer) C-S-H and portlandite may determine the shrinkage of the paste. In Fig. 9, the amount of amorphous phase instead of C-S-H is plotted as the amount of portlandite. As it is confirmed by Fig.9, through the hydration process, the ratio of portlandite to amorphous is almost constant in both L and N pastes, however, the ratio is varied between L and N pastes. It seems that difference of the ratio caused by mineral or phase composition of each cement. Therefore, it is possible to show the different trend between shrinkage strain and amorphous phase amount. As a result, it is concluded that drying shrinkage of cement paste can be explained by the amount of amorphous and the ratio of the amount of portlandite to the amount of amorphous phase.

4. CONCLUSIONS

In the present contribution, drying shrinkage of cement paste, which is affected by the age of start of drying and mineral composition of used cement, is investigated. Based on the experimental results, the following conclusions are derived;

(1) Drying shrinkage of cement paste is increased as the age of start of drying is increased. And the drying shrinkage of cement paste using low hear Portland cement is larger than that of cement paste using ordinary Portland cement paste. This trend is consistent in cases of different relative humidity conditions and different age of start of drying.

(2) There is a linear relationship between amount of amorphous phase and drying shrinkage strain. Larger amount of amorphous phase, whose major component is calcium silicate hydrate, in cement paste corresponds to the larger shrinkage strain. But the trends of paste using ordinary Portland cement (N) and low heat Portland cement (L) was not the same.

(3) The reason of the different relationship between amount of amorphous phase and shrinkage strain for L and N can be explained by the different ratio of amount of portlandite to the amount of amorphous phase. Based on the previous research, portlandite in paste is considered to contribute to restrain the colloidal agglomeration of outer C-S-H which is the major factor of irreversible shrinkage under the the first desorption process

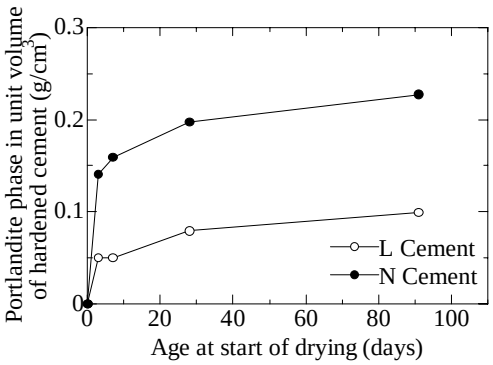

Fig. 8 Relationship between mass of portlandite of L and N and age at start of drying.

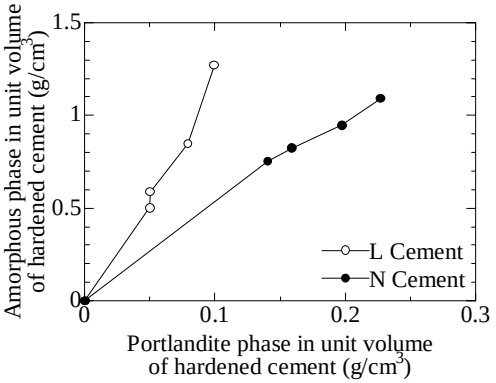

Fig. 9 Amount of amorphous phase in L and N paste as a function of portlandite amount.

ACKNOWLEDGEMENT

Partial works of the present experiments are sponsored by JSPS KAKENHI Grant Number 15H04077, and collaboration research between Nagoya Univ. and NIPPO co.

REFERENCES

[1] Architectural Institute of Japan, “Japanese Architectural Standard Specification for Reinforced Concrete Work JASS5 2009.”

[2] Ministry of Land, Infrastructure, Transport and Tourism, “Criteria for removal of moulds and struts of the cast-in-place concrete based on the provisions of the Building Standards Law’s construction example of Artcle 76 in second paragraph.”

[3] S. Tsukioka, “Effect of stripping time of concrete form and environmental humidity on compressive strength of concrete with Portland blastfurnace slag cement,” Journal of the Agricultural Engineering Society, Japan, Vol.58, 1990, No.12, pp.1199-1204.

[4] I. Maruyama, H. Sasano, “Strain and crack distribution in concrete during drying,” Materials and Structures, Vol.47, 2014, pp.517-532.

[5] H.S. Wong, M. Zobel, N.R. Buenfeld, R.W. Zimmerman, “Influence of the interfacial transition zone and microcracking on the diffusivity, permeability and sorptivity of cement-based materials after drying,” Magazine of Concrete Research, Vol.61, 2009, pp.571-589.
[6] C. Aldea, S. Shah, A. Karr, “Effect of Cracking on Water and Chloride Permeability of Concrete,” Journal of Materials in Civil Engineering, Vol.11, 1999, pp.181-187.
[7] I. Maruyama, H. Sasano, Y. Nishioka, G. Igarashi, “Strength and Young's modulus change in concrete due to long-term drying and heating up to 90 °C,” Cement and Concrete Research, Vol.66, 2014, pp.48-63.
[8] S. Nagamatsu, Y. Sato, Y. Ohtsune, “Relationship between degree of drying and drying shrinkage strain of hardened cement paste (in Japanese),” Journal of structural and construction engineering, 1992, pp.13-21.
[9] P. Stutzman, S. Leigh, “Phase Composition Analysis of the NIST Reference Clinkers by Optical Microscopy and X-ray Powder Diffraction,” NIST Technical Note 1441, 2002, pp.34-43.
[10] Fachinformationzentrum Karlsruhe and National Institute of Standards and Technology, “Inorganic Crystal Structure Database, ICSD,” 2006, (http://icsd.ill.fr/icsd/index.html).
[11] I. Maruyama, G. Igarashi, “Cement Reaction and Resultant Physical Properties of Cement Paste,” Journal of Advanced Concrete Technology, Vol.12, 2014, pp.200-213.
[12] I. Maruyama, H. Sasano, Y. Nishioka, G. Igarashi, “Strength and Young's modulus change in concrete due to long-term drying and heating up to 90 °C, Cement and Concrete Research, Vol.66, 2014, pp.48-63.
[13] I. Maruyama, Y. Nishioka, G. Igarashi, K. Matsui, “Microstructural and bulk property changes in hardened cement paste during the first drying process,” Cement and Concrete Research, Vol.58, 2014, pp.20-34.
[14] I. Maruyama, N. Kishi, A. Teramoto, G. Igarashi, “Effect of mineral composition of Portland cement on shrinkage property (in Japanese),” Proceedings of Japan Concrete Instituite, Vol.32, 2010, pp.347-352.
[15] I. Maruyama, G. Igarashi, Y. Nishioka, “Bimodal behavior of C-S-H interpreted from short-term length change and water vapor sorption isotherms of hardened cement paste,” Cement and Concrete Research, Vol.73, 2015, pp.158-168.
[16] S. Goto, M. Daimon, G. Hosaka, R. Kondo, “Composition and Morphology of Hydrated Tricalcium Silicate,” Journal of the American Ceramic Society, Vol.59, 1976, pp.281-284.
[17] P.D. Tennis, H.M. Jennings, “A model for two types of calcium silicate hydrate in the microstructure of Portland cement pastes,” Cement and Concrete Research, Vol.30, 2000, pp.855-863.
[18] M. Jensen, P. F. Hansen, “Autogenous Deformation and Change of the Relative Humidity in Silica Fume-Modified Cement Paste,” ACI Materials Journal, Vol.96, 1996, pp.539-543.